Available online at www.sciencedirect.com

ScienceDirect

journal homepage: www.elsevier.com/locate/he

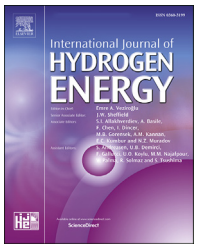

Recent advancements in hydrogen storage - Comparative review on methods, operating conditions and challenges

Subrajit Bosu, Natarajan Rajamohan *

Chemical Engineering Section, Faculty of Engineering, Sohar University, Sohar, PC 311, Oman

HIGHLIGHTS

- Detailed review on hydrogen storage methods is presented.
- Role of cryogenics and adsorptive media are discussed.
- The comparative performance of various methods is tabulated.
- Existing research gap and future perspectives are analyzed.

ARTICLE INFO

Article history:
Received 18 July 2022
Received in revised form
25 January 2023
Accepted 28 January 2023
Available online 17 February 2023

Keywords:
Hydrogen
Storage
Adsorption
Nanomaterials
Energy
Efficiency

ABSTRACT

Green hydrogen, proposed as a sustainable alternative for conventional fuels, has gained utmost importance due to its reduced carbon footprint and potential application in maintaining balance between energy generation and demand. Utilization of hydrogen-based systems are challenged by cost effective storage methods. Bio-hydrogen storage technologies using cryogenic and adsorptive methods are discussed in this review paper, along with their operating conditions and storage capacities. An analysis of operational challenges and recent advancements in hydrogen storage techniques is presented. With a storage pressure of 70 MP, cryogenic hydrogen is almost twice as dense as compressed hydrogen. Technical challenges such as material cost and explosion risk can be addressed by hydrogen adsorption on activated carbon active sites. Maximum hydrogen storage capacity are reported by activated carbon obtained from Chitosan (6.77 wt%), Bamboo (6.6 wt %) and African palm shell (6.5 wt%) at 77 K and 4–20 Mpa. Further, nanotechnology approaches are presented in detail for increasing hydrogen storage capacity in pristine Si and Mg. The future perspectives in terms of technological, and economic aspects are discussed.

Introduction

Energy supply and demand requires a sustainable approach to ensure continuous development of industries and infrastructure. Two significant global concerns faced are climate change and soaring energy consumption. Sustainable technologies and the use of renewable energy can reduce greenhouse gases, oxides of Nitrogen/Sulphur and carcinogens emissions. This strategy can simultaneously contribute to the economic and social development of global population in the long run. There has been a dramatic escalation in oil prices for traditional power plants. In consequence, the corresponding volatility in energy prices has an impact on

* *Corresponding author.*
E-mail address: rnatarajan@su.edu.om (N. Rajamohan).
https://doi.org/10.1016/j.ijhydene.2023.01.344

economic development and sustainability [1–4]. The efficiency and technologies of renewable energy enable us to offer low-carbon energy that is abundant, reliable, clean, safe, and independent of fuel prices. As an eco-friendly and sustainable energy source, hydrogen is a great alternative to fossil fuels. A fuel like gasoline or another fossil fuel has an energy density that is approximately seven times lower than a fuel like hydrogen. The increased energy density of hydrogen makes it a more desirable fuel. The safety and special measures required for the transport and storage of hydrogen have a major impact on the application and widespread use of hydrogen. Currently, transportation is fueled primarily by petroleum refinery fuels [5–7]. Petroleum fuels, however, are becoming increasingly expensive and hard to come by. Hydrogen can fill this niche perfectly. To use this fuel as a transportation fuel, however, high-density storage channels must first be developed [8–10].

Hydrogen can be stored in several ways, including high-weight tanks (350–700 bars) that have a high capacity. It is still low compared to conventional energy sources despite the pressure. In order for storage tanks to hold high-pressure conditions, they should be constructed from solid and light-weight materials. Hydrogen fuel storage strategies in the future for vehicles is cryogenic liquefaction of atomic hydrogen. Dehumidification of hydrogen is a serious challenge due to the transfer of ambient heat. The internal storage pressure increases and results in a major cause of fuel losses, such as boil-off. Since hydrogen can be absorbed in metal solids (such as Li, Mg, or Al) via dissociation, storing solid compounds chemically is a safer and more efficient method than liquefying them. Hydrogen can be restored on a large scale using this method under ambient conditions of temperature and pressure. The general structural energy of a material is determined by its specific gravity. The high endothermic enthalpy of hydrogen requires high temperatures to desorb it from its parent material. In consequence, the material is less energy-efficient than it could be. The storage of chemical hydrogen is usually carried out at low temperatures and high pressures. There are still a few problems to be solved regarding chemical storage, even though it has many potential benefits. Due to its structural and thermal instability, the material is unstable at constant temperatures and pressures. To address these challenges, we need adsorbents with high porosity. For example, the effectiveness of physisorption adsorbents mainly influenced by the surface properties [11–18]. With this background, the main objectives of this review paper are to (i) describe various modes of hydrogen storage techniques (ii) review the cryogenic applications and their operating conditions (iii) review the applications of activated carbon, characterisation techniques used and the operating conditions (iv) nanotechnology approach in hydrogen storage (v) future perspectives.

Modes of hydrogen storage

The most widely used hydrogen storage techniques includes physical storage and chemical storage. Fig. 1 presents the various modes of hydrogen storage, focussing on physical and chemical principles.

Physical

A compressed gas storage system is the most adopted method for H_2 storage technology. In suitable cylinders, hydrogen can be compressed and stored as pressurized gas, with a pressure of up to 700 bar, in containers or even in underground caverns. As a high-pressure gas, hydrogen has the advantage of

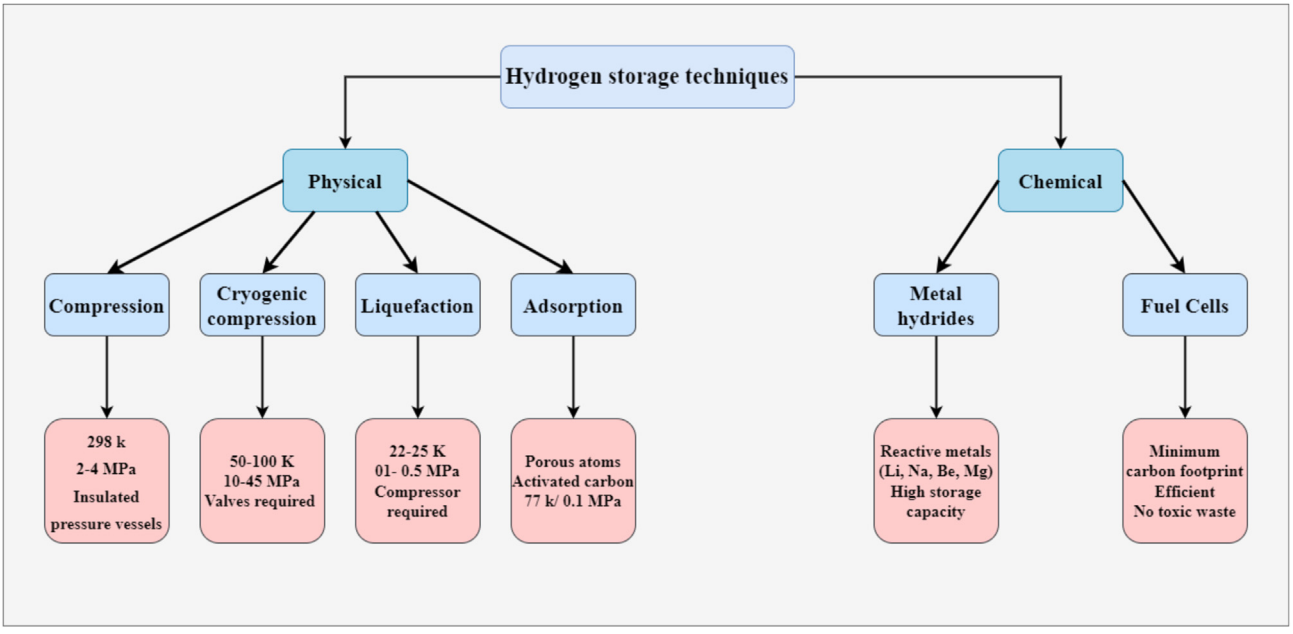

Fig. 1 – Modes of Hydrogen storage.

simplicity, and the ability to fill and release quickly. As a result of the real gas behaviour of hydrogen, the volumetric density of such a storage system remains constant regardless of the pressure [19–22]. Cryogenic liquids are typically stored in liquid H_2 tanks rather than tanks designed to withstand internal pressure. The volume and mass of insulation usually represent a minimal percentage of H_2 volume in cryogenic hydrogen tanks. Liquid hydrogen is not as mobile as gas hydrogen due to its thermodynamics. Despite the low storage temperature of 20 K, boil-off losses are a primary concern. To protect liquid H_2, tanks must be heavily insulated, which means they have thick walls. The use of liquid hydrogen is suitable where high energy density is required but boil-off is not a problem [22–25]. H_2 is compressed using a combination of compressed gas and liquid H_2. This process is known as cold/cryogenic compression. For a cryogenic tank to withstand internal pressure, it must be able to hold a cryogenic fluid. The cryo-compression process does not require as many high strength materials as 700 bar room-temperature storage. It's normal to insulate using a vacuum and to contain pressure using high-strength materials, which are not always rare or harmful [22,25–29]. H_2 adsorption on carbon materials has been observed to have a superior storage capacity when compared to absorption. Adsorption of hydrogen can be enhanced by porous materials, which reduces hydrogen storage amounts significantly. As hydrogen molecules don't form chemical bonds with the carbon atom on the surface, hydrogen is stored on activated carbon through physisorption, which is a physical phenomenon. Carbon nanotubes, carbon nanofibers, and activated carbon all exhibit the highest H_2 storage capacities for hydrogen adsorption. It is necessary to have a pressure of 750 bars at 298 K to store 4.1 kg H_2, but only 150 bars at 77 K. If activated carbon pellets are added to the container, the pressure is further reduced to 60 bar [30,31].

Chemical

The chemical hydrogen storage material classification generally refers to compounds that are covalently bonded to hydrogen atoms. H_2 storage materials made from complex metal hydrides are light weight and fairly compact. The absorption of H_2 forms ionic or covalent compounds in complex metal hydrides. Hydrogen gas can be used to form solid state compounds with lighter metals than Magnesium such as Sodium, Lithium, and Beryllium. Gravimetric hydrogen capacities can be increased due to their light weight and the fact that they typically have two atoms per metal atom [32–36]. Metal borohydrides ranged in gravimetric and volumetric capacities from 14.9 to 18.5 wt % and 9.8–17.6 MJ/L. Statistically significant results were obtained. Studies of $LiBH_4$ were particularly extensive. The hydrogenation and dehydrogenation of $LiBH_4$ took place at high temperatures with slow kinetics [37–42]. A hydrogen-rich ionic liquid with a low molecular weight can be used as a storage medium. The recently identified parameters with reference to new ionic liquid compounds are temperature of operation, purity and release velocity of hydrogen. Under both thermal and catalytic conditions, an ionic liquid of methyl guanidinium borohydride released 9.0 wt% H_2. A guanidinium octahydrotriborate compound was reported to be formed by combining guanidinium cation with an octahydrotriborate anion [43–45].

Studies on hydrogen storage and their operating conditions

This section presents the overview of various research studies focussing on physical and chemical methods for hydrogen storage, the operating conditions used and the related thermodynamic aspects.

Compression/liquefaction

A hybrid energy storage system using compressed air and hydrogen was recently developed using physical methods aimed at storing hydrogen. Through the thermal integration of two sub-systems, large amounts of energy can be stored in pressure tanks with limited volume. A thermodynamic analysis of this integrated hybrid system has been conducted. This technology is competitive with intensively developed pure hydrogen energy storage technologies based on the assumed parameter values, which resulted in a storage efficiency of 38.15%. In comparison to the hybrid system, three reference systems, each using hydrogen generators, produced similar results. Typical Power-to- H_2 to-Power systems combine hydrogen generators with fuel cells. Compressed air energy storage is also used in those two systems. During the charging stage, compressed air/hydrogen storage systems use a relatively small amount of energy to fuel the air compressor. A compressed air tank can reduce the requirement for storage volume and can therefore be an alternative solution to the problem in places where underground storage tanks aren't feasible [46].

High thermal endurance and high storage density are two advantages of cryo-compressed containers for automotive applications. Hydrogen's cooling powers are wasted during the venting and discharge processes. An innovative venting method which used a throttling valve is presented in this research for cryo-compressed hydrogen storage. When parking, discharging and driving hydrogen in a vessel, different initial pressures, release pressures, and filling amounts are studied. With a throttling valve of 2 MPa release pressure in the vessels, parking time can be extended by 55%. When a vessel has a high filling density and a long parking time, the recovering cooling capacity will increase the parking time a lot. Different hydrogen storage pressures are simulated during drive simulations. Through throttling, the reduction in upper limit of operating pressure is achieved and leads to a reduction in investments. Cooling-recovery venting can have considerable thermodynamic benefits when used during driving. Cryo-compressed hydrogen storage systems are designed and optimized in this study [47].

The insulation of the pressure vessels also allows for the storage of hydrogen at higher pressures without the risk of overpressure. This makes it possible to store the same amount of hydrogen in a smaller volume, increasing the efficiency of the storage system. Furthermore, insulated pressure vessels are easy to transport and can be used for a variety of applications, such as fuel cell vehicles and stationary fuel cell

systems. It is possible that these advantages could exceed the complexity of simultaneously requiring a cryogenic insulation vessel and a high-pressure vessel. Vessels with composite wrapping and aluminum lining safety has been evaluated through a variety of tests. Cryogenic operations do not weaken vessels, as indicated by both experiments and analysis. Pressure vessels that are insulated have been extensively tested and can now be seen in operation onboard a vehicle. The vessel was placed in an enclosed chamber at a temperature of 333 K with a humidity of 95% and cycled from zero to service pressure 5000 times. The vessel was shut off after cycling with a temperature of 221.9 K and an air temperature of room temperature. During the second round, 30 times of recycling between zero and service pressure was completed. A burst test was then conducted. No misshaping, or fluid loss was observed during the cycling pressurization test [48].

The cryogenic storage of hydrogen is characterized by a dynamic model and capable of storing both liquids and compressed H_2 at 350 bar. To ensure that the tank can be refuelled frequently, regardless of initial conditions, a double-flow refuelling device is used. When liquid hydrogen is loaded into the tank, the H_2 is classified as supercritical fluid if it reaches a temperature of >120 K and as subcooled liquid, if it reaches a temperature of <100 K. In order to maintain a sufficient pressure inside the tank, an in-tank heater must be installed. As liquid H_2 is withdrawn from its supercritical state, it transforms into a two-phase mixture and eventually into a superheated gas. Hydrogen can be efficiently delivered if the minimum pressure is met and the heater's power rating is high enough. How long cryogenic hydrogen can sit in a tank depends on storage pressure and maximum allowable pressure. If the evaporative losses do not exceed 64% of the theoretical capacity, the hydrogen cannot be drained from the tank [49].

With cryogenic pressure vessels incorporated into a high pressure system, high density hydrogen can be stored without evaporative losses, like that of liquid hydrogen. With less carbon fibre, comparatively more storage can be achieved. The lightweight design and ability to refuel quickly make them suitable for both long and short trips. Cryogenic hydrogen is used for longer trips while compressed hydrogen is used for shorter ones. System performance and thermal endurance improves as the size of the cryo-compressed hydrogen storage system grows. Slim, large-sized storage systems can achieve the highest system energy densities. A simplified thin insulation can achieve optimal thermal endurance for vessels with larger diameters and limited extensions when volume-to-surface ratios are optimized. As such, a given design space may constrain the design of the vessel and the insulation, while also allowing room to balance costs and optimize the integration of the vehicle while optimizing system performance. Compared to traditional liquid hydrogen tanks, thermal endurance of the studied vessel is 5–10 times greater, and evaporative losses are reduced as well [50].

The on-board performance and high-volume production cost for methane reforming method were tested in high pressure tanks operating at 350 and 700 bar respectively. It is hard to meet the Well-to-Tank efficiency target with the 350-bar system, whereas 700-bar system comes close by about 5%. Because compressed gas hydrogen storage systems have a relatively large footprint, dual-tank systems offer package flexibility over single-tank systems. Single-tank vessels must have approximately 25% thicker walls than the low-pressure vessels. Due to the increased thickness, the lower surface area of each tank is nearly counterbalanced. Therefore, double-tank systems cost less than 5% more than corresponding single-tank systems [51].

With a single H_2 tank and a cryogenic pressure vessel, the longest distance driven was 1050 km. With a volume of 135 L and a capacity of 9.3 kg of liquid hydrogen, the tank operated at a maximum pressure of 245 bar. An internal combustion engine powered by hydrogen was installed onboard the vessel. Over the course of 20 months, 11 experiments were completed, each lasting between 1 and 2 months. They took place on full-scale vessels. The experimental procedures start with regenerating a vacuum using a turbomolecular pump. A large vessel made oven baking impractical, despite its desirable properties. A heating tape was used instead of the vacuum jacket to warm the vessel to 323 K. Three days of temperature control were achieved with the use of a vacuum pump. When the vessel cooled to ambient temperature, the vacuum pump was still running. The heat transfer rate is found to be relatively constant between 20 K and 120 K at 4.5–5 W. Lower vacuum quality compensates for the higher heat transfer rate, and both effects are nearly cancelled in this regime. Heat transfer increases to 6 W between 120 K and 170 K, due to the vacuum effect. Heat transfer drops to its minimum value of 4 W as the temperature rises to 170–270 K without corresponding increases in vacuum pressure [28].

A recent study investigated two different liquefaction processes to determine the optimized conditions in order to reduce the specific liquefaction costs. Process 1 is a high-tech process that produces liquid hydrogen (LH_2) at close to 6 kWh per kg with significant decrease in cost of liquefaction. By comparison with conventional liquefiers, both process and equipment have been optimized for scaling-up; a closed loop mixed refrigerant cycle is used to precool hydrogen, and a modified Claude cycle with turbine energy recovery is used to precool hydrogen. In order to meet higher liquefaction needs, Process 2 with two separate cryogenic cycles was proposed. Turbo compressors are used in the new hydrogenation mixture cycle. With a 100 tpd hydrogen liquefier, very high reduction in liquefaction costs was achieved, in comparison to a conventional 5 tpd hydrogen liquefier. If the liquefaction capacity is increased from 5 to 50 tpd hydrogen, 60% reduction was achieved [52].

The development and evaluation of a cryogenic liquefaction process for hydrogen are presented. The process is reported to produce 300 tons of liquid hydrogen per day using two independent refrigeration cycles and mixed refrigerants. It uses the least power energy of the identical liquefaction plants in its second cooling cycle, which cools the hydrogen to 20 K with a power consumption of 3.258 kWh/kgL H_2. In the proposed process, refrigerants are mixed based on the configuration of heat exchangers and expanders, which is a novel approach. From an energy and energy perspective, the proposed process is analyzed. According to the energy analysis, the proposed process has a coefficient of performance of 0.1797, which makes it more efficient than other identical processes. A detailed analysis of exergy efficiency shows that

the exergy efficiencies of 67.53%, 52.24%, and 55.47% were achieved first, second and whole process respectively [53].

The hydrogen refuelling stations of fuel cell electric vehicles can be transported in tube trailers filled with compressed gaseous hydrogen. Various distances, tube trailer configurations, and payloads were considered in the study in order to evaluate hydrogen transport costs. Steel tube trailers are restricted by weight regulations and can carry only 270 kg of hydrogen while composite tube trailers can carry 1100 kg of hydrogen at 500 bar. The rapid increase in vessel weight that results from thick walls is counterproductive when transporting hydrogen at high pressure in steel pressure vessels. Composite tube trailers with a 3-by-3 array of 30-inch-diameter vessels are the most economical. A linear relationship between the deliverable payload and the capital cost is required when developing configurations with the lowest cost-per-unit payload. An estimated $1100 is required to deliver one kg of hydrogen payload. When smaller vessels are packed in greater numbers on a trailer, payload is higher and H_2 delivery costs are lower, especially for hydrogen delivery to large hydrogen stations. A tube trailer configured with the proper hydrogen payload can reduce hydrogen delivery costs by up to 16% [54]. Table 1 presents the applications of various physical methods used for hydrogen storage, the operating conditions and the thermodynamic observations.

Adsorption on activated carbon

A variety of industrial applications related to gas sorption are suited to activated carbons due to their desirable surface characteristics. The search for alternative low-cost precursor feedstocks will always be necessary to reduce production costs. A rapid carbonization procedure successfully synthesized mesoporous and microporous carbon materials from honey vine-milkweed as a sustainable carbon source from biowaste. With 4.5% phosphorus, the carbon exhibits 1.75 wt% H_2 uptake capability at 298 K and 100 bar. In P-PC, doping and porosity could combine to explain this phenomenon. When the current density is 1 A/g, it exhibits a 253 F/g specific capacitance. Activated carbon exhibits high stability during repeated use, enhanced retention capacity (95% over a period of 10,000 cycles) and reduced impedance. The recent focus on energy storage methods shifted towards biowaste -derived material with favourable surface properties. Nitrogen, sulphur, and boron, for example, are heteroatoms that present additional polar sites in a carbon network. Carbon and electrolyte ions can synergistically interact. In aqueous (alkaline, acidic) electrolytes, porous carbon doped with phosphorus is more likely to exhibit good storage capacity because it can become hydrophilic due to oxidized P-atoms. This allows good contact of ions with the electrode surface [59].

Rice husks have been used to create activated carbon materials for hydrogen storage, which have been chemically activated by KOH. Research study has investigated the hydrogen storage behaviour of rice husk based activated carbon and the influence of activation medium and size of the pores were examined. It was determined that the textural properties of activated carbons could influence hydrogen storage in rice husk-based hydrogen storage materials by correlating their properties with hydrogen storage properties. The micropore volume and distribution of pores 0.6–0.8 nm in size, which are crucial for hydrogen physisorption on KOH activated samples, developed as expected. A rice husk to KOH ratio of 1:1 resulted in the highest micropore volume, 0.792 cm^3/g, and the hydrogen storage capacity, 2.85 wt%, at 0.1 MPa. The best structural properties were found when the KOH rate was 3 or 4 for the synthesis of activated carbons using existing KOH. Injecting hydrogen until the system reaches 1 bar of pressure after it has been cooled to room temperature. Hydrogen that is ultra-high pure (99.9%) minimizes influences of moisture or impurities on measurement [60].

An advanced three-step synthesis method was developed, involving the synthesis of carbon precursors followed by the synthesis of activated carbon at 77 K. Nitrogen-doped activated carbon (NAC-1.5-600) absorbed 2.96 wt% hydrogen. Activated carbon derived from synthetic materials has so far shown the highest uptake. Optimum pores with diameters of 0.59 nm (large pore volume) contributed to the high uptake of NAC-1.5-600. At 77 K, it appears that the ultra-micropore volume is the primary adsorption mechanism. However, at higher pressure, pores larger than 1 nm, as in NAC-1.5-700, also contribute to hydrogen adsorption. Hydrogen adsorption at 77 K hardly depends on nitrogen, oxygen, and hydrogen content. Based on the increase in hydrogen adsorption on activated carbons, higher pressures are likely to lead to higher uptake. Narrow pores exhibit stronger surface - hydrogen interactions because the potential fields of both sides of the pores overlap. As a result of stronger interactions in ultra-micropores, the heat of adsorption is higher, increasing hydrogen storage capacity [61].

To improve hydrogen storage properties and textural properties of melaleuca bark-based porous carbon, scientists chemically activated the porous carbon to modify its surface properties. For activation, different doses of KOH were used to test the effect of different KOH concentrations on product porosity. The microstructures of carbon materials as obtained and their hydrogen storage properties have been analyzed in detail. Furthermore, it is examined how the structure influences the hydrogen storage capacity and the size and area of pore spaces. Understanding hydrogen adsorption factors might be gained through this investigation. At 77 K and 10 bar, these samples showed high surface areas of 3170 m^2/g as well as large hydrogen storage capacities of 4.08 wt%. In this study, surface area, pore volume, and H_2 adsorption capacities were shown and compared across samples. Similarities can be seen between the H_2 adsorption capacity, micropore volume, and surface area. Therefore, H_2 adsorption capacity is related to the degree to surface area and volume of micropores. Therefore, at 77 K and 10 bar, the higher the surface area and micropore volume of the samples, the greater the H_2 adsorption capacity [62].

A porous carbon prepared from Palimera sprouts is tested for its hydrogen storage capabilities using KOH activation. A KOH activation process produces a higher yield and less activation energy than other activation processes. Porous carbons obtained from such processes exhibit well-defined pore distributions and their specific surface areas can reach 3000 m^2/g. A large surface area and a wide distribution of pore sizes are features of porous carbon material under investigation. Considering this aspect, porous carbon is an ideal material to examine the impact of the two parameters mentioned

Table 1 – Physical methods and their operating conditions for hydrogen storage.

Technique	Temperature/K	Pressure/Mpa	Thermodynamic Analysis	Process units	Life cycle assessment	References
Compression	298.0	4.000	Atmospheric air 288 K, a pressure of 101.325 kPa and humidity of 60%/ Electromechanical efficiency of the compressor = 98%	Hydrogen Generator/ Methanation Unit/ Heat Exchanger/ Fluid compressor/ Hydrogen Tank	Medium energy storage efficiency/High technological maturity/ No harmful substance emission/No heat storage	[46]
Cryogenic compression	50–100.0	10–45.000	The parking time of 1 MPa vessels is 14% greater than that of 35 MPa vessels/ 50 MPa vessels have 416% more parking time than 2 MPa vessels/With a throttling valve, 1600 kJ of cooling can be utilized in less than 500 h	Insulated storage tanks/Throttling valves	75% ortho-hydrogen and 25% parahydrogen used as raw materials/ Recycle continues until the hydrogen in the vessel is below 1 kg	[47]
Cryogenic compression	219.9	0.101	With the vessel filled to a maximum of 84% with liquid hydrogen at 20 K and 1 atm, the container has an internal volume of 84 L/5 kg of hydrogen is stored in the tank/The vessel has a heat transfer rate of 1 W/ 95% air humidity	Insulated pressure vessel/ Thermocouples/ Liquid level sensor/ Temperature sensor	Tank dormancy is 5 days/Thirty cycles were performed on the vessel/Vessel was tested for cryogenic drop and fill.	[48]
Cryogenic compression	100–120.0	35.000	The tank is uniformly heated and pressurized/ Optimal delivery pressure at 8 bar and 31 K	Heat exchanger/ Vent valve/fill valve/ Heater/Flow controller	Tank storage capacity is 64%/Dormancy can go beyond 40 Wd//Double flow recycling installed	[49]
Cryogenic compression	45–50.0	25.000	Adiabatic system/ Maximum mechanical energy of 0.55 kWh/kg	Heat exchanger/ pressure vessels/ valves	Increased cost of composite wrapping for insulated vessels/ Recycling done for maximum storage capacity	[50]
Compression	233.0	70.000	Maximum volumetric capacity is 27.5 g H_2/L /Isentropic efficiency is 88%/Mechanical efficiency 97%/	Temperature sensor/ Pressure gauge/ Valve/Compressor	80% production/4% pipeline delivery/16% storage/14.8 kg.CO_2/kg H_2 emission	[51]
Cryogenic compression	30–60.0	20–87.500	There is a net heat transfer from tank/ Constant heat transfer rate of 5 W	Insulated pressure vessels/Fill valves	10.4 kg tank storage capacity/Efficient range for vehicle/Cheapest acquisition cost/ Enhanced safety	[28]
Liquefaction	22.80	0.200	Specific energy consumption of 5.9 –6.6 kWh/kg liquid H_2/Liquefaction increases by 40% at ambient pressure.	Mixer/Valves/ Pressurized vessels/ Compressor	Cost reduction by 67%/ 20 years plant operation/95% plant availability	[52]

(continued on next page)

Table 1 – (*continued*)

Technique	Temperature/K	Pressure/Mpa	Thermodynamic Analysis	Process units	Life cycle assessment	References
Cryogenic liquefaction	20–78.0	2.100	1.102–3.258 kWh/kg power consumption/ Pump and compressor have 90% exergy efficiency/53.84% process rational efficiency	Separator/Mixer/ centrifugal pump/ Compressor/Cooler/ Reactor	Efficient liquefaction/ Requires lower pressure and less compressors/ Lower cost of production	[53]
Compression	233.0	50.000	Efficient system/ Thermodynamically Feasible.	Pressure vessel/ Compressor/ refrigeration unit/ dispenser	16% reduced delivery cost/Capital cost of $1100/kg H_2	[54]
Cryogenic compression	36–83.0	50.000	Pressure and temperature in the storage vessel are uniform/Thick insulation lowers heat loss to 10 W/ 72% volumetric efficiency	Insulated tank/ Condenser/Pressure and temperature transducer/Solenoid Valves	7day dormancy/System cost reduced by 21%/ 15,000 cycles of exhaustion life	[27]
Cryogenic compression	30–60.0	87.500	Net heat transfer from pump/Total 68 kg Boil off losses due to warm up/No need for precooling.	Valve/pressurized tank/pumps/ Pressure gauge/ rupture discs/ pressure transducer	Exceptional back-to-back refills/Minimal power demand/no detectable deterioration/Easy to maintain/Minimum carbon footprint	[55]
Cryogenic compression	24.60	34.5–87.500	Maximum fill density/Efficient storage capacity/ Specific internal energy of 10kJ/kgK	Heat exchanger/ Insulated tanks/ Valves	Low capital cost/ Inexpensive refuelling	[56]
Cryogenic compression	10–100.0	25–35.000	85% fibre efficiency/ 4 W heat transfer rate from vessel/ 100 km/kg H_2/ Minimum vent losses	Pressure vessel/ Pumps/Pressure and temperature sensors	Lower storage cost/ increased durability/ Vessel material withstands high pressure	[57]
Cryogenic compression	35–110.0	5–70.000	In the total energy consumption, 41% of it comes from latent heat/Hydrogen cools almost linearly above its critical temperature	Refrigerator/Cooler/ storage tank/ compressor	High storage lifespan/ Fast tank filling/lower installation cost	[58]

above. Hydrogen storage studies and electrochemical measurements were conducted to quantify the hydrogen storage capacity. An electrolyte solution of 1 M H_2SO_4 was used as the electrolyte in a three-electrode cell for cyclic voltammetry measurements, which confirmed that the storage mechanism is based on the mechanism of physisorption and is fully reversible. Studies using the Sievert's apparatus, built locally, were conducted on high-pressure physical storage. Electrochemical experiments can be conducted at room temperature and atmospheric pressure, while the electrochemical set-up is more complex. Adsorption experiments on hydrogen indicated a good hydrogen uptake capacity of 1.06 wt% at a pressure of 15 bars and a temperature of 298 K [63].

Under different experimental conditions, microwave irradiated African oil-palm shell was used to prepare activated carbons. Various irradiation conditions were studied, which established that exposure at 800 W for 15 min gave the best hydrogen storage capacity in the activated carbon sample. Using this material for an activation process with LiOH to develop porous textures suitable for hydrogen storage is a novel attempt. The formation of functional groups can result from the reaction between LiOH and carbon precursors, based on thermodynamic considerations. While the char is being activated, the Li and O bonds will cause the adjacent lamella to oxidize, which will lead to the formation of cross-linking carbon atoms. The lamella is divided into surface functional groups by the edges. The crystallite is changed from flat shape to folded pattern due to the removal of crosslinking between adjacent lamella. Furthermore, the lithium metal that is produced during the activation process is incorporated into the

lamellae of the crystallite in situ. By washing the carbon material with water, the lithium salts in the carbon particles are leached out. Due to the irreversible change, voids are created between layers [64].

The hydrogen adsorption degree of activated carbon (AC) was investigated using Arundo donax. The activated carbon from Arundo donax synthesized at of 77, 273.15, and 298 K respectively, was found to absorb 12.87 mg/g, 0.11 mg/g, and 0.09 mg/g of hydrogen, respectively. The activated carbon with an activated surface area of 1784 m^2/g and a mesopore volume of 98.38% developed by zinc chloride, exhibited good hydrogen adsorption performance. These results indicate that ACs with a controlled pore size distribution may be useful for the adsorption of H_2. Hydrogen storage at near room temperature has become increasingly desirable for operational reasons, but physisorption hydrogen uptakes in activated carbons are usually very small at ambient temperatures, and notable hydrogen storage can only be observed at very high pressures. The hydrogen uptake capacity of AC was 0.11 mg/g at 273.15, and 0.09 mg/g at 298.15 K under pressure of 805 mmHg. This value can be increased at higher pressures [65].

A method to prepare porous carbon materials was developed recently using biomass pyrolysis method and calcium citrate. The method utilized the vapours released by biomass pyrolysis before condensation and produced light bio-oil that was of high quality via co-production after condensation. Carbon materials are formed by complex reactions between pyrolysis vapours and calcium citrate during carbonization, creating oxygen-rich functional groups on the surface. Carbon-containing precursors lose weight during carbonization according to a five-stage reaction kinetic model. Carbon material prepared under optimum working conditions possesses maximum surface area (1703 m^2/g), a relatively high micropore volume of 0.51 cm^3/g, and a 24.17% microporosity. Hydrogen can be adsorbed at a greater capacity than many other absorbents at 77 K, at atmospheric pressure and presented in Table 2. In light bio-oils prepared at higher temperatures with carbon-containing precursors, it can be seen that the concentration of acids and alcohols gradually decreased, while ketones and phenols gradually increased. The light bio-oil obtained from 323 K precursor preparation contains the most acids with 32.69% [66].

The KOH activation method was used to prepare activated carbon samples with high porosity based on Litchi trunks. By wetness impregnation and acidic oxidation, respectively, oxidized-AC and Pd-AC samples were prepared. A study of the hydrogen adsorption effects of a porous texture, functional groups, and catalysts of ACs was conducted. It was found that oxygen-hydrogen molecules interacted more strongly than carbon–hydrogen molecules. As the acidic group amounts increased, the micropore volume decreased. Acidic groups acting as steric hindrances on the AC surface resulted in fewer hydrogen molecules entering the micropores due to the steric hindrance effect. It is also possible that the ACs were destroyed due to their microporosity after the excess-oxygenation treatment. In contrast, the hydrogen was unable to bind to the acidic functional groups on the surface of AC. A critical component of hydrogen storage was the microporous structure of carbon [67].

Carbon nano porous materials with surface areas up to 3000 m^2/g have been shown to have a gravimetric density of 4.7 wt% when under high pressure, following chlorination of TiC under 600C and activation under CO2, or synthesizing CDCs (carbide-derived carbons) at low temperatures (673 or 773 K) and activation under KOH. Even though mesopores (1 nm or smaller) can adsorb hydrogen efficiently and contribute to an increased adsorption temperature, they do not contribute significantly to hydrogen storage in these conditions. Based on sample analysis, it was found that pore size does not affect the surface of carbon in the same way as functional groups. When the specific surface area and the pore volume are higher, the hydrogen can be absorbed more effectively. The requirement of narrow size distribution with open pores is necessary for high-pressure hydrogen storage at cryogenic temperatures in carbon materials to achieve high hydrogen uptake, according to research., The surface chemistry was reported to have an insignificant influence on pore size, as hydrogen uptake did not increase [68].

Chemically activated hydrocarbon materials were used to form highly porous carbons. At 77 K, these porous carbons exhibit superior hydrogen storage performance, having hydrogen uptake capacities of 1.75–2.71 wt per cent and 4.23–6.77 wt percent at 1 bar and 20 bar, respectively. Additionally, high levels of N-doping are beneficial for hydrogen storage at low pressure but can negatively affect hydrogen storage at high pressure. Carbons with low N - doping have no appreciable impact on hydrogen uptake, however. The activated adsorbent exhibits the highest hydrogen uptake (6.77 wt %), which may be due to its ultra-micropore surface area. It seems that porous carbons can be used as hydrogen storage candidates if one is able to enhance porosity with a high surface area associated with an optimal distribution of pore sizes [69]. Table 2 presents the applications of activated carbon, characteristics of activated carbon and the storage capacity.

Silicon and magnesium-based nanomaterials for hydrogen storage

There is a great deal of interest in semiconductor devices using silicon, a leading and multifaceted material. Non-crystalline and polycrystalline Si have a high affinity for hydrogen, making them suitable for hydrogen storage. In addition to their geometric, photonic, electromagnetic, and thermodynamic properties, silicon-derived nanostructures including Si nanowires and porous Si quantum dots have unique properties [83–87]. Room-temperature hydrogen storage materials are crucial to establishing a hydrogen economy. With diatom frustules as sources of silicon, a novel nanomaterial to store hydrogen can be synthesized. This nanomaterial can achieve approximately 5% hydrogen storage capacity at 298 K and 20 bar H_2 equilibrium pressure. A nano matrix has been formed by encapsulating graphene plates within micropores of Silica. An average of 50–100 mg of diatom frustules can be found in the nanomaterials. Pd–Co/DG is a novel hydrogen-sorption material composed of a stable bimetallic alloy composed of Pd_3Co on a nano-matrix with a surface area of 163.25 m^2 per gram and a pore volume of

Table 2 – Characteristics of activated carbon employed for hydrogen storage and the storage capacity.

Precursor	Temperature/K	Pressure/Mpa	Preparation time/hr	Hydrogen storage capacity/wt%	Characterisation techniques	Micropore volume/cm^3g^{-1}	Specific surface area/m^2g^{-1}	Size/nm	Reference
Honey vine milkweed	298.0	10.0	18	1.75	XRD/RS/FT-IR/EDAX/XPS/HRTEM/SEM	0.300	756.000	1.35	[59]
Rice husks	77.0	0.1	24	2.85	XRD/TGA/XPS/SEM	0.792	2232.000	05–0.90	[60]
1,3 bis(cynomethyl imidazolium) chloride	77.0	0.1	24	2.94	XPS/TEM	0.26–1.160	526–2386.000	0.5–0.70	[61]
Melaleuca bark	77.0	1.0	36	4.08	XRD/SEM/TEM FTIR/XPS/HRTEM	0.860	3170.000	2–3.00	[62]
Palimera sprout	298.0	1.5	16	1.06	XRD/TEM/HRTEM/SEM/RS/CV	1.440	2090.000	1–2.00	[63]
African palm shell	77.4	15.0	48	6.50	TGA/FTIR	0.480	1350.000	0.70	[64]
Arundo donax	77–298.0	0.1	170	1.30	FTIR/EDS	0.880	3870.000	297000.00	[65]
Light biomass oil	77.0	0.1	50	1.53	SEM/TEM/FTIR	0.510	1703.000	5.00	[66]
Litchi trunk	303.0	6.0	30	0.53	FTIR	1.790	3400.000	20–100.00	[67]
Synthetics	77.0	6.0	18	2.63	NLDFT/BET	0.650	1481.000	0.90	[68]
Chitosan	77.0	2.0	13	6.77	NLDFT/BET/SEM/HRTEM	0.67–1.497	1362–3009.000	0.6–0.80	[69]
Bark/Camellia shell	77–87.0	0.1	10	3.01	XPS/SEM/NLDFT/BET	1.080	2849.000	0.7–1.70	[70]
Coal fly ash	77.0	0.1	14	1.35	EDS/XRF/SEM/XRD	0.477	946.770	1000.00	[71]
Polyaniline	77–100.0	6.0	12	5.50	SEM/SAXS/RS/EIS/CV	1.000	2200.000	500.00	[72]
Bagasse	123.0	0.1	24	2.13	XRD/RS/SEM	1.010	2243.000	2.39	[73]
Bamboo	77.0	4.0	15	6.60	TGA/XPS/EA/FTIR/HRTEM/XRD/SEM	1.010	3208.000	1.08–1.65	[74]
Olive Pomace	77.0	20.0	12	6.11	Quenched solid density functional theory/ BET/SEM/TEM/XRD	0.270	0.021	<0.70	[75]
Almond shells	77–298.0	2.7–4.7	25–30	2.53	FTIR/SEM/EDX/BET/DFT/NLDFT	1.660	1307.000	40.00	[76]
Onion	77.0	0.1	36–48	3.67	EIS/CV/XPS/XRD/TGA/TEM/SEM/RS	1.390	3150.000	1.05–1.08	[77]
Lignin	77.0	0.1	6–10	1.80	Gel permeation chromatography/NLDFT/ PXRD/RS/XPS	0.42–0.520	1064–1258.000	0.70	[78]
Fruit Bunch	77.0	2.0	4	2.14	SEM/BET/FTIR	0.297	687.000	1.9–2.40	[79]
Waste tyres	77.0	0.10	75	1.40	EDS/XRD/FTIR	0.145	955.2	0.86	[80]
Poly (vinylidene chloride)	20.4–303.0	0.1–20.0	12–24	6.50	BET	2–0.46	1021–2760.000	0.53–2.54	[81]
Jute fibres	303.0	4.0	50	1.20	XRD/SE/BET/FTIR	0.740	380–1224.000	0.5–1.50	[82]

BET: Brunauer– Emmett–Teller method; CV: Cyclic Voltammetry; EDX: Energy dispersive X-ray; FAAS: Flame atomic absorption spectroscopy.
FESEM: Field emission scanning electron microscopy; FTIR: Fourier-transform infrared spectroscopy; HRTEM: High resolution transmission electron microscopy; NLDFT: Non local density functional theory; RS: Raman spectroscopy; SEM: Scanning electron microscopy.
TGA: Thermogravimetric analysis; XPS: X-ray photoelectron spectroscopy.

0.84 cm^3 per gram. TEM images reveal an average particle size of 12 nm whereas the elemental composition shows the designed nanostructure exhibits oxygen contamination in the matrix [88].

An analysis of the H_2 adsorption properties of several metals decorated on porous silicon was conducted. Li and Pd are well bonded to the pores, while Be is not. The maximum number of hydrogen molecules that Li or Pd can adsorb is five and four, respectively. There is either too much distance between them or too small adsorption energy above this number. H_2 molecules are adsorbed to the surface of the be atom during chemisorption. Adsorbent metals have strong chemisorption properties, which are critical for H_2 physisorption. Surface H atoms passivated the surface to enhance chemisorption. To accomplish this, the metal was attracted by an electromagnetic field. Consequently, an effective charge region influenced the electronic density of H_2 molecules. Out of the three examined decorating atoms, lithium emerged as the most effective due to its strong chemisorption to pore walls, higher H_2 adsorption energies, parallel sorbate-sorbent orientation, and lighter atomic weight [89]. A tetrahedral silicon carbide monolayer could be improved by using density functional theory. A Li, Na, and Mg atom decoration strategy was used to achieve this. To begin with, pure silicon carbide (SiC) crystallographic and electrochemical qualities were assessed. Furthermore, different orientations of the hydrogen molecule H_2 were tested at different adsorption sites with respect to its adsorption energy stability on the pristine SiC surface. To determine what configuration would be most stable during the adsorbed state of the H_2 molecules, this was done. Several metal concentrations were used at the preferred location to confirm the stability of the nanocomposite. Li, Na, and Mg monolayers with decoration can adsorb up to 24 molecules of hydrogen H_2 per atom. An electrostatic charge is generated when reactive metallic elements and SiC surfaces have a significant difference in electronegativity. This may increase the stability of the hydrogen molecule H_2 and increase its affinity for binding to other molecules. As a result, Li–SiC, Na–SiC, and Mg–SiC have gravity densities of 6.50 wt%, 5.54 wt%, and 5.48 wt%, respectively [90].

As much as 6.6% by weight of interfacially trapped hydrogen has been demonstrated to exist in porous silicon. An electrochemical etching process carried out in hydrofluoric acid readily results in hydrogenated porous silicon. Temperatures as high as 280C can cause hydrogen gas to be released thermally. The desorption temperature of silicon may be reduced, and gaseous recharge of the matrix may be improved by a suitable catalyst at the pore mouth. Researchers present a kinetic study of reversible hydrogen storage through porous silicon based on the mechanisms of dissociation, spill over, and bond jumping. These steps were followed by determinations of a vibrational frequency and activation energy value for each step. The activation energies and vibrational frequencies determined from the microlevel DFT study were used to assess the kinetic performance of catalytically modified porous silicon as a hydrogen storage material. The difference between full and empty charges is determined by comparing atomic calculations to macroscopic calculations. They demonstrate rapid recharge at 8 bar using a proton-exchange membrane fuel cell waste heat equivalent to that of a proton-exchange membrane fuel cell [91].

Because of its abundance, high uptake ability, and non-toxicity, functionalised Mg nanomaterial is also seen as a promising hydrogen storage material along with Si. Various carbon materials can be grown in situ by the facile chemical solid-state method with magnesium hydride nanoparticles. The enclosed templates are made from commercial carbon materials, such as coconut shell charcoal (CSC). MgH_2 nanoparticles can grow on its large surface because of the layering and interconnected wrinkles in its structure. Nanoparticles of MgH2 can also be contained within CSC because of their porous structure with an average diameter of 3.8 nm. Furthermore, CSC is amorphous in nature. Ball-milling of amorphous CSC can result in destabilizing the Mg–H bonds and diffusing hydrogen atoms due to the increased defect sites. Within 10 min, 5.4 wt percent of hydrogen could be released from the nanostructures. Over the course of 2 h, 5.8 wt% of hydrogen can be desorbed. Hydrogen (5 wt%) can be absorbed by the nanocomposite in 5 min at 523 K and 2 MPa. Dehydrogenation occurs at 598 K at 0.09 wt% per minute, and hydrogenation occurs at 523 K at 3.01 wt% per minute [96].

Two-dimensional Ti_3C_2 grafted MXene sheets encapsulated on Ni have been used in a recent study as a catalyst. Liquid-state reduction of Ni onto exfoliated MXene sheets in a liquid-state reduction process resulted in their successful synthesis. The hydrogen sorption properties of MgH_2 were catalysed by this compound when it was introduced into a ball milling system. MgH_2 hydrosorption kinetics were improved with the application of a nano additive as a catalyst. As a result of a local increase in irradiation-induced temperature in a vacuum, it is known that magnesium hydroxide can decompose when irradiated with electron beams in a vacuum. Having conducted an in-situ TEM study, we were able to determine the structure of the hydrogen desorption process using a 3 nA irradiation current. This allowed researchers to perform a more detailed analysis of microstructure evolution. At 398 K, the nanocomposite can act as a catalyst for the absorption of 5.4 wt% H2 in 25 s as well as for the release of 5.2 wt % H_2 in 15 min at a temperature of 523 K, resulting in a positive net gas exchange. A study has shown that even at room temperature, it can absorb volumes of hydrogen within 5 h, regardless of temperature. There is also a dehydrogenation peak temperature of 494 K on the composite, which indicates a high degree of dehydrogenation [97].

To enhance the hydrogen storage properties of Mg, TiC (Titanium carbide) nanoparticles were grafted in 2–3 nm carbon shells through a reactive gas evaporation method. By adjusting the evaporation rate of Mg and Ti, the average particle size of Mg–TiC nanocomposite (NC) is controlled below 50 nm, and the content of TiC is adjusted between 4 and 25 wt %. NC is capable of rapidly absorbing 5.5 wt% hydrogen within 25 min at 523 K and desorbing 4.5 wt% hydrogen within 60 min at 573 K with a loading percentage of 88%. At 523–573 K, ten hydrogenation/dehydrogenation cycles remain stable for hydrogen storage capacity and kinetics. It is thought that the enhanced hydrogen storage kinetics of the nanocomposite are due to the synergistic effects of the carbon confinement nanostructure and the nonstoichiometric TiC catalysis. When the amount of TiC in the reaction chamber increases, the

intensity of its diffraction peak increases as well. Argon plasma produces Ti vapor, which when combined with C atoms formed by decomposing CH_4 forms TiC. Low concentrations of H2 make Ti difficult to evaporate. Hence, TiC cannot be formed at low H_2 concentrations due to Ti's rapid evaporation [98]. Table 3 presents the details on various Silicon and magnesium nanostructures designed for hydrogen storage. Fig. 2 represents the mechanism of hydrogen storage onto Silicon and magnesium nanostructures.

Challenges in hydrogen storage

Gases at atmospheric pressure have a much too low volumetric storage density for any practical use. The only onboard storage for a car that is feasible is gaseous hydrogen at high pressure. Currently, the most sophisticated system available is a composite vessel capable of withstanding 70 MPa, which is used by several prototype vehicles. When pressures are drastically reduced, volumetric storage density becomes inadequate. As such high pressures are quite noticeable, further boosting the pressure does not appear to be helpful. A composite vessel is comprised of an interior liner based on high density polymers that are impermeable to hydrogen, a shell made up of carbon fiber and polymer to withstand pressure, and an outer layer of polymers that provide impact resistance. Spherical shapes are ideal for withstanding high pressures at minimal weight. As a result, the cylindrical shape with two hemispheric end caps is technically used in a car since this would create extreme packaging challenges [101].

It is difficult to create a liquid hydrogen tank system. Vacuum insulation is added to the tanks and radiation shields are incorporated to minimize heat influx, especially when feedthroughs are present in the domes. The manufacturing of such tanks is possible, but they can be quite expensive. A drawback of liquefied hydrogen is that liquefaction uses a lot of energy. In comparison with hydrogen gas compression, it costs approximately 30% more energy. In addition, it is not possible to recover the liquefaction energy during operation. Liquefaction does use a lot of energy, but considering its integration into an overall system, the disadvantage may not be so severe. A filling station needs to deliver the hydrogen or it must be generated on site [102]. Because of the intrinsic low adsorption enthalpy of hydrogen on porous carbon, it is difficult to store large amounts of hydrogen at room temperature, although large quantities of hydrogen can be stored at cryogenic temperatures. This means that H_2 is an alternative energy that cannot be used at room temperature. H_2 has relatively weak physical contact with solid surfaces because it doesn't have a charge, has no dipole moment, has a relatively inadequate quadrupole moment, and has a weak polarizability [103]. Metal hydrides are another option for storing hydrogen. Most hydrides cannot be used for this. This is the result of either too high or too low decomposition temperatures, insufficient volumetric or gravimetric storage capacity. Furthermore, recovery of these hydrides is intractable due to the difficulty in reversing the dehydriding reaction. Before they can be reused, chemical hydrides have to be dehydrated and then processed off-board. To release hydrogen from chemical hydrides, a large quantity of water may be required, which can create a storage system volume problem. For hydrogen storage to be widely accepted, these challenges must be overcome. As a powder, metal hydride has a particle size range of 5–20 μm, but after repeated hydriding and dehydriding cycles, the particle size tends to decrease. The hydrogen atoms within the metal hydride matrix cells occupy the interstitial sites during the hydriding reaction, causing the matrix cell to expand. Metal hydrides therefore possess low effective thermal conductivity [104]. There is no economic viability for hydrogen until it is affordable in comparison to conventional fuels. Hydrogen's cost is largely determined by its storage costs. A fixed charge of the capital cost accounts for about 62% of the costs associated with hydrogen liquefaction in large plants. Next, power consumption and operations and management costs account for 30% and 8%, respectively. It is estimated that hydrogen liquefaction currently costs about $1.11 per kilogram of liquid hydrogen, and costs are to be reduced to $0.53 by US hydrogen program [105,106]. Compressed gas vessels cost more as they operate at higher pressures and have greater capacities. At 140 bars, a vessel operates at $400 per kg of stored hydrogen and at 540 bars, it costs about $2100 per kg. It may also cost about $13,000 for cylindrical steel tanks with a capacity of 765 L and operating at around 415 bars. Therefore, compressing a kilogram of H_2 costs about $650, compared to approximately $500 for storing compressed natural gas. There can be a wide range of capital costs associated with cryogenic storage vessels, ranging from $20/kg to $4500/kg, depending on storage capacity. A compressed hydrogen tank costs considerably less than a liquid hydrogen tank for short-term storage. As compared to compressed hydrogen storage, the long-term storage of hydrogen as liquid may offer a cost advantage. There is a great deal of variation in price between storage vessels for metal hydrides. There is a capital cost of $4200/GJ to $18,400/GJ associated with metal hydrides, as well as a storage cost of $2.90 to $7.00/GJ associated with metal hydrides [107,108]. Fig. 3 presents the challenges in hydrogen storage. The merits and demerits of hydrogen storage applications by chemical and physical means are summarized in Table 4.

Future perspectives

A wide range of fuel cell applications is possible in the future due to the improved performance of hydrogen storage materials. Commercial fuel cell vehicles will be developed at a large scale as a result of the breakthrough in hydrogen storage. In order to optimize reversible hydrogen absorption and dehydrogenation performance, researchers should use an efficient approach that combines catalytic doping and structural modification, which may yield a synergistic effect. The use of simulation software coupled with machine learning applications should be designed to provide an accurate description of lifecycle analysis. Among these will be advection, molecular gaseous diffusion, and mechanical distribution of particles. In addition, software developed should consider multiphase-multi materials flow conditions within a heterogeneous reservoir. The model will account for thermal deviations of injected hydrogen, the mixing of several gas components, and

Table 3 – Silicon and magnesium nanostructures designed for hydrogen storage.

Precursor	Chemicals used	Hydrogen storage capacity/wt%	Physicochemical parameters	Thermodynamic parameters	References
Diatom-frustule/ graphene	Pd_3Co/Graphite oxide/ H_2SO_4/HNO_3/$PdCl_2$/ $CoCl_2$	4.83	• Micropore volume 0.84 cm^3g^{-1} • Specific surface area 163.25 m^2g^{-1} • Average particle size 12 nm	• Temperature 298 K • Pressure 2 MPa • Isosteric heats of adsorption 20.4 kJ/mol	[88]
Li–Pd/porous silicon	Crystalline Si/LiH_2/solid Pd	0.34	• Si and Pd form a covalent bond with high strength • Large charge density of Pd causes rapid H_2 adsorption • Lithium chemisorbs H2 effectively parallelly	• Formation energy for Li –Si interaction –3.15 eV • Li–Si binding energy –3.05 eV • 0.265 eV adsorption energy for Li–Si	[89]
Li–SiC Na–SiC Mg–SiC	Silicon carbide nanotubes/Graphene/ pure metals	6.5 5.54 5.48	• The bond angles for Si –C–Si is 86° and 94.01° for C–Si–C • Lattice constant is 11.83 Å	• Sorption temperature range 178–186 K • Dehydrogenation entropy 130 $J\ K^{-1}\ mol^{-1}$ • Mean sorption energy of Li–SiC = –0.258 eV, Na –SiC = –0.244 eV, Mg –SiC = –0.247 eV	[90]
Hydrogenated porous silicon	Crystalline silicon/Pd/H_2	6.6	• Pore diameter 1.75 nm • Lattice constant is 5.43 Å	• $E_{adsorption}$ is 1.81 eV • Bond hopping energy barrier is 2.06 eV • Optimum storage capacity at 8 bar	[91]
Ni-doped silicon carbide	$(SiC)_{16}$/Ni ore	0.43–0.50	• Designed nanocage more effective sorbent than pristine C_{60} • Ni–Si bond length 2.24 Å	• $E_{adsorption}$ is 0.7 eV • $E_{binding\ energy}$ is-0.737 eV • Optimum temperature 298 K	[92]
8B transition metal functionalised SiC	SiC/single walled carbon NT/Ru/Os/Co/Rh/Ir	0.93	• Bond length 1.811 Å • Bond angles of Si–TM –Si is 87.3–105.3 eV	• $E_{adsorption}$ is –14.07 kcal/mol • E_{HOMO} –5.252 eV • E_{LUMO} –5.252 eV • $E_{adsorption}$ .13.42 kcal/mol • E_{gap} = 2.095eV	[93]
$Cu_3(BTC)_2$/Si	$CaSi_2$/NaOH/Crystal Si/ Methanol/Sodium Dodecyl sulphate/$SnCl_2$/ N, N-dimethylformamide/ $Cu(NO_3)_2$	5.6	• Lamellar thickness of 9.52 nm • Crystal lattice distance is 0.312 nm • 362 m^2/g specific surface area • Exhibits octahedral nanostructure	• Reversible storage at 77 K and 4 MPa	[94]
Al–Si/porous silicon	Si powder/HNO_3/ Ethanol/deionised water/HCl/Ni	0.81	• Specific surface area 218.8 m^2/g	• Optimum H_2 adsorption at 0.1 MPa and 77 K • Al facilitates hydrogen sorption of Si nano powder	[95]
MgH_2	Coconut shell charcoal/ Carbon nanotubes/ Graphite/activated carbon/$MgCl_2$	5.4	• Solid phase method employed • 3.8 nm average pore diameter • Specific surface area 1090 m^2g^{-1} • Pore volume 13.5 cm^3g^{-1}	• Free energy 75.06 kJ/mol • $E_{activation}$ is 120 $kJmol^{-1}$ • Optimum pressure 2 Mpa	[96]

(continued on next page)

Table 3 – (*continued*)

Precursor	Chemicals used	Hydrogen storage capacity/wt%	Physicochemical parameters	Thermodynamic parameters	References
MgH_2/2D-Ni@Ti_3C_2	MXenes/Ti_3AlC_2/HCl/NaOH/H_2O	5.4–4	• Particle size <1 nm confirmed by TEM images. • XRD peak at 44° due to Ni proves it's effective catalytic behaviour	• Desorption temperature 816 K • $E_{activation}$ is 141–73 kJ/mol • Isothermal sorption/desorption employed 10 times at 298 K and 3 MPa	[97]
Mg/TiC	Pristine Ti and Mg/H_2/CH_4/Coal	5.5	• Lattice constant is 4.326 Å • Pore diameter 37 nm • Hydrogen release and bond formation can occur on TiC	• Desorption enthalpy is −74.7 kJ/mol H_2 • $E_{activation}$ is 54.7 $kJmol^{-1}$ • Optimum hydrogen adsorption at 573-523 K and 4 Mpa	[98]
Mg–V composite	Molten Mg/Pure V/Ar/N_2/H_2	5	• Particle diameter 50 −150 nm. • BET surface area 20.5 m^2g^{-1}. • Lattice constant 5.211 Å	• Optimum hydrogen adsorption at 473–623 K and 4 Mpa • $E_{activation}$ is 71.2 $kJmol^{-1}$ • $E_{decomposition}$ of nano-particles is −74.5 $kJmol^{-1}$	[99]
MgH_2/$MgFe_2O_4$	$Mg(NO_3)_2 \cdot 6H_2O$/$H_4N_2 \cdot H_2O$/Mg/Deionised water/$Fe(NO_3)_3 \cdot 9H_2O$	5.5	• Crystal size 19 nm	• $E_{activation}$ is 99.9 $kJmol^{-1}$ • Gibbs Free energy −1317 $kJmol^{-1}$	[100]

the heterogeneity of actual reserves. New hierarchical materials should be designed in the future with high strength to withstand the infiltration and cycling of the hydrides [117,118]. Further, developing in-situ synthesis techniques for enhancing micropore geometry will be the key to finding more efficient hydrogen storage systems. Also, it is necessary to study how dissociated hydrogen atoms are transported onto receptor surfaces. Enhanced hydrogen storage techniques and adsorbents at ambient temperatures can be enhanced with a deeper understanding of surface chemistry. Recent years have seen significant advancements in magnesium's ability as a promising candidate for hydrogen storage. Although its hydriding and dehydriding temperatures are high, its kinetics are poor, which hinders its potential uses. A large amount of in-depth research needs to be conducted on magnesium interlayer nanocomposites and external layer functionalization using other metals. As a result, the kinetics of desorption will be accelerated and temperatures will be feasible [119,120]. In addition, Al based hydrides (alanates) also possess H_2 storage properties with high capacity but again more frequent

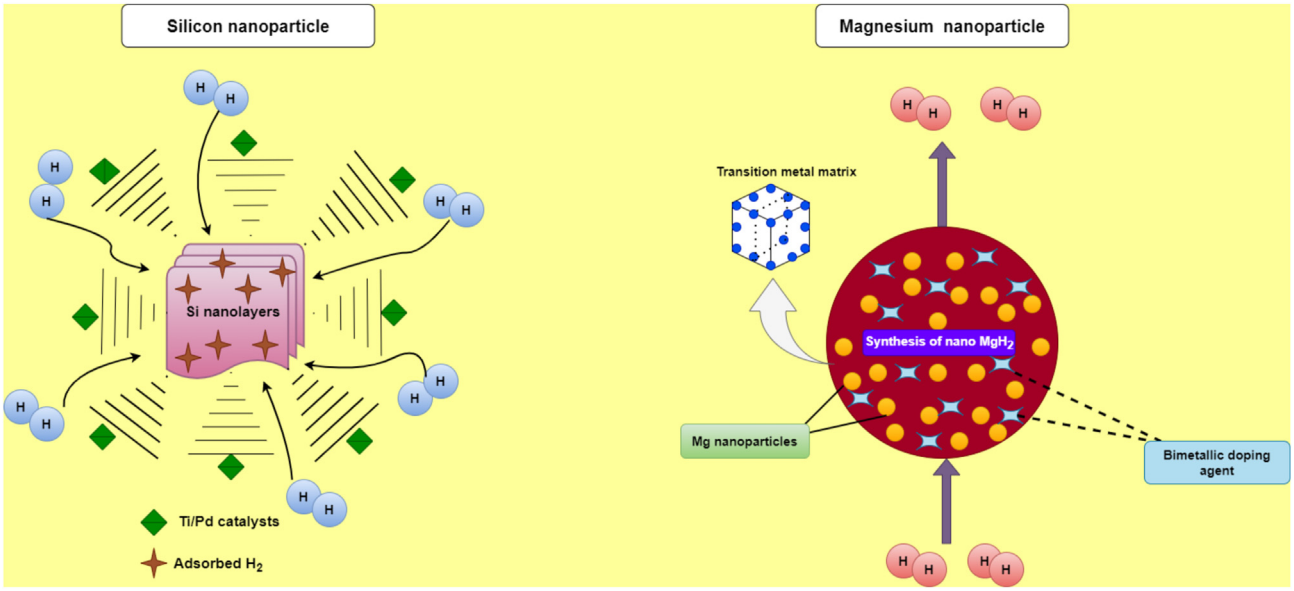

Fig. 2 – Mechanism of hydrogen storage onto Silicon and magnesium nanostructures.

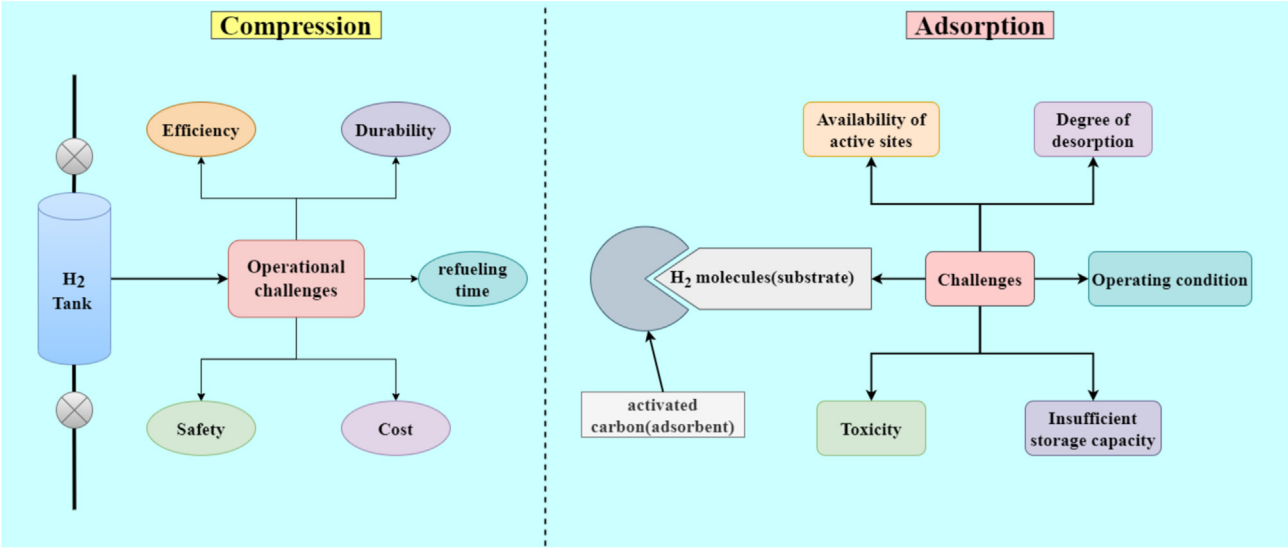

Fig. 3 – Challenges in hydrogen storage.

Table 4 – Merits and demerits of hydrogen storage techniques.

Methods	Merits	Demerits	References
Liquefaction	• A high level of purity. • There is no need to dehydrogenate and purify this fuel.	• In the process of liquefaction, about 15% of the hydrogen's energy is consumed. • Stores poorly for long periods of time and hydrogen is lost through evaporation • Regulation of boil off is needed • Liquid leakage risk	[109,110]
Cryogenic compression	• Energy density of hydrogen is exceptional • An efficient volumetric system • Enhanced gravimetric measurement capability	• Extremely low operating temperature • A technical challenge lies in managing thermal conditions • High energy cost	[111,112]
Adsorption	• 23% reduction in hydrogen storage volume with compression at 20 MPa and 298 K • Due to its exothermic nature, this process is favored by low temperatures and high pressure • Adsorbent is relatively cheap	Technical issues in temperature regulation Majority of adsorbents are poor thermal conductors	[113,114]
Metal hydrides	• Physical compression requires higher temperatures and pressure, so this method is safer. • The thermal drive of compression simplifies heat management	• Less efficient • Compression elements with expensive alloys are more expensive • The sorption/desorption kinetics of metal hydrides are affected by poisoning by gas mixtures	[115]
Fuel cells	• Efficient • Sustainable • No need of charging	• Expensive materials used for redox reaction	[116]
Porous silicon	• Faster uptake kinetics • Storage capacity >5 wt% most cases	• Prone to surface oxidation • Low desorption volume • Weak reversibility	[85,87]

experiments needed to be performed to evaluate it's thermodynamics and improve sorption/desorption performance by alterations to the structure [121]. There is a need for in-depth studies on the properties of organic and inorganic nanomaterials to identify their storage capacity and to analyse how does heat transfer parameters affect adsorption site on nano substrates.

Conclusion

This study has explored the recent developments in cryogenic compression, liquefaction and utilizing functionalised adsorbent materials for storage of hydrogen. Hydrogen storage capacities are found to be influenced by the operating

pressure and temperature, under cryogenic conditions. The details on process units employed and the life cycle assessment are summarized. In addition, the applications of activated carbon, synthesized from a variety of feedstocks, are reviewed for their suitability to store hydrogen. Biomass based activated carbon yielded acceptable storage efficiencies and are more favored due to their eco-friendly properties and lower cost. The various surface characterisation techniques employed for activated carbon are reviewed and surface functionalization related heterogeneity is reported to enhance the hydrogen adsorption properties. Also, the BET surface area and operating temperature are found to influence the storage capacity. Thus, this review article has presented a detailed summary on the merits and de-merits of the cryogenic and adsorptive methods for hydrogen storage. The future scope for improving the storage capacity and efficiency was discussed. Technology based on hydrogen storage holds the potential to change the way we power our homes, our transportation systems, and even our daily lives. Despite this, both academics and manufacturers still have a great deal of work ahead of them to realize and exploit the potential and benefits of the hydrogen economy.

Declaration of competing interest

The authors declare that they have no known competing financial interests or personal relationships that could have appeared to influence the work reported in this paper.

REFERENCES

[1] Montoya FG, Aguilera MJ, Manzano-Agugliaro F. Renewable energy production in Spain: a review. Renew Sustain Energy Rev 2014;33:509–31. https://doi.org/10.1016/j.rser.2014.01.091.

[2] Kumar A, Kumar K, Kaushik N, Sharma S, Mishra S. Renewable energy in India: current status and future potentials. Renew Sustain Energy Rev 2010;14(8):2434–42. https://doi.org/10.1016/j.rser.2010.04.003.

[3] Klessmann C, Rathmann M, de Jager D, Gazzo A, Resch G, Busch S, Ragwitz M. Policy options for reducing the costs of reaching the European renewables target. Renew Energy 2013;57:390–403. https://doi.org/10.1016/j.renene.2013.01.041.

[4] Nilsson M. Red light for Green Paper: the EU policy on energy efficiency. Energy Pol 2007;35(1):540–7. https://doi.org/10.1016/j.enpol.2005.12.023.

[5] Becherif M, Ramadan HS, Cabaret K, Picard F, Simoncini N, Béthoux O. Hydrogen energy storage: new techno-economic emergence solution analysis. Energy Proc 2015;74:371–80. https://doi.org/10.1016/j.egypro.2015.07.629.

[6] Eberle U, Felderhoff M, Schueth F. Chemical and physical solutions for hydrogen storage. Angew Chem Int Ed 2009;48(36):6608–30. https://doi.org/10.1002/anie.200806293.

[7] Schlapbach L, Züttel A. Hydrogen-storage materials for mobile applications. In: Materials for sustainable energy: a collection of peer-reviewed research and review articles from nature publishing group; 2011. p. 265–70. https://doi.org/10.1142/9789814317665_0038.

[8] Rowsell JL, Yaghi OM. Strategies for hydrogen storage in metal–organic frameworks. Angew Chem Int Ed 2005;44(30):4670–9. https://doi.org/10.1002/anie.200462786.

[9] Yang J, Sudik A, Wolverton C, Siegel DJ. High capacity hydrogen storage materials: attributes for automotive applications and techniques for materials discovery. Chem Soc Rev 2010;39(2):656–75. https://doi.org/10.1039/B802882F.

[10] Panella B, Hirscher M, Roth S. Hydrogen adsorption in different carbon nanostructures. Carbon 2005;43(10):2209–14. https://doi.org/10.1016/j.carbon.2005.03.037.

[11] Collins DJ, Zhou HC. Hydrogen storage in metal–organic frameworks. J Mater Chem 2007;17(30):3154–60. https://doi.org/10.1039/B702858J.

[12] Singh R, Altaee A, Gautam S. Nanomaterials in the advancement of hydrogen energy storage. Heliyon 2020;6(7):e04487. https://doi.org/10.1016/j.heliyon.2020.e04487.

[13] Zhou L. Progress and problems in hydrogen storage methods. Renew Sustain Energy Rev 2005;9(4):395–408. https://doi.org/10.1016/j.rser.2004.05.005.

[14] Dong J, Wang X, Xu H, Zhao Q, Li J. Hydrogen storage in several microporous zeolites. Int J Hydrogen Energy 2007;32(18):4998–5004. https://doi.org/10.1016/j.ijhydene.2007.08.009.

[15] Germain J, Fréchet JM, Svec F. Nanoporous polymers for hydrogen storage. Small 2009;5(10):1098–111. https://doi.org/10.1002/smll.200801762.

[16] Yang SJ, Jung H, Kim T, Park CR. Recent advances in hydrogen storage technologies based on nanoporous carbon materials. Prog Nat Sci: Mater Int 2012;22(6):631–8. https://doi.org/10.1016/j.pnsc.2012.11.006.

[17] Wang H, Gao Q, Hu J. High hydrogen storage capacity of porous carbons prepared by using activated carbon. J Am Chem Soc 2009;131(20):7016–22. https://doi.org/10.1021/ja8083225.

[18] Hu B, Wang K, Wu L, Yu SH, Antonietti M, Titirici MM. Engineering carbon materials from the hydrothermal carbonization process of biomass. Adv Mater 2010;22(7):813–28. https://doi.org/10.1002/adma.200902812.

[19] Yamashita A, Kondo M, Goto S, Ogami N. Development of high-pressure hydrogen storage system for the Toyota "Mirai" (No. 2015-01-1169). SAE Technical Paper; 2015. https://doi.org/10.4271/2015-01-1169.

[20] Gye HR, Seo SK, Bach QV, Ha D, Lee CJ. Quantitative risk assessment of an urban hydrogen refueling station. Int J Hydrogen Energy 2019;44(2):1288–98. https://doi.org/10.1016/j.ijhydene.2018.11.035.

[21] Zhang F, Zhao P, Niu M, Maddy J. The survey of key technologies in hydrogen energy storage. Int J Hydrogen Energy 2016;41(33):14535–52. https://doi.org/10.1016/j.ijhydene.2016.05.293.

[22] Rivard E, Trudeau M, Zaghib K. Hydrogen storage for mobility: a review. Materials 2019;12(12):1973. https://doi.org/10.3390/ma12121973.

[23] Xu W, Li Q, Huang M. Design and analysis of liquid hydrogen storage tank for high-altitude long-endurance remotely-operated aircraft. Int J Hydrogen Energy 2015;40(46):16578–86. https://doi.org/10.1016/j.ijhydene.2015.09.028.

[24] Babac G, Sisman A, Cimen T. Two-dimensional thermal analysis of liquid hydrogen tank insulation. Int J Hydrogen Energy 2009;34(15):6357–63. https://doi.org/10.1016/j.ijhydene.2009.05.052.

[25] Petitpas G. Simulation of boil-off losses during transfer at a LH2 based hydrogen refueling station. Int J Hydrogen Energy

2018;43(46):21451–63. https://doi.org/10.1016/j.ijhydene.2018.09.132.
[26] Moreno-Blanco J, Petitpas G, Espinosa-Loza F, Elizalde-Blancas F, Martinez-Frias J, Aceves SM. The fill density of automotive cryo-compressed hydrogen vessels. Int J Hydrogen Energy 2019;44(2):1010–20. https://doi.org/10.1016/j.ijhydene.2018.10.227.
[27] Ahluwalia RK, Peng JK, Roh HS, Hua TQ, Houchins C, James BD. Supercritical cryo-compressed hydrogen storage for fuel cell electric buses. Int J Hydrogen Energy 2018;43(22):10215–31. https://doi.org/10.1016/j.ijhydene.2018.04.113.
[28] Aceves SM, Petitpas G, Espinosa-Loza F, Matthews MJ, Ledesma-Orozco E. Safe, long range, inexpensive and rapidly refuelable hydrogen vehicles with cryogenic pressure vessels. Int J Hydrogen Energy 2013;38(5):2480–9. https://doi.org/10.1016/j.ijhydene.2012.11.123.
[29] Ahluwalia RK, Hua TQ, Peng JK, Lasher S, McKenney K, Sinha J, Gardiner M. Technical assessment of cryo-compressed hydrogen storage tank systems for automotive applications. Int J Hydrogen Energy 2010;35(9):4171–84. https://doi.org/10.1016/j.ijhydene.2010.02.074.
[30] Mohan M, Sharma VK, Kumar EA, Gayathri V. Hydrogen storage in carbon materials-A review. Energy Storage 2019;1(2):e35. https://doi.org/10.1002/est2.35.
[31] Paggiaro R, Bénard P, Polifke W. Cryo-adsorptive hydrogen storage on activated carbon. I: thermodynamic analysis of adsorption vessels and comparison with liquid and compressed gas hydrogen storage. Int J Hydrogen Energy 2010;35(2):638–47. https://doi.org/10.1016/j.ijhydene.2009.10.108.
[32] Lototskyy MV, Yartys VA, Pollet BG, Bowman Jr RC. Metal hydride hydrogen compressors: a review. Int J Hydrogen Energy 2014;39(11):5818–51. https://doi.org/10.1016/j.ijhydene.2014.01.158.
[33] Jain IP, Lal C, Jain A. Hydrogen storage in Mg: a most promising material. Int J Hydrogen Energy 2010;35(10):5133–44. https://doi.org/10.1016/j.ijhydene.2009.08.088.
[34] Song Y. New perspectives on potential hydrogen storage materials using high pressure. Phys Chem Chem Phys 2013;15(35):14524–47. https://doi.org/10.1039/C3CP52154K.
[35] Jain IP, Jain P, Jain A. Novel hydrogen storage materials: a review of lightweight complex hydrides. J Alloys Compd 2010;503(2):303–39. https://doi.org/10.1016/j.jallcom.2010.04.250.
[36] Sakintuna B, Lamari-Darkrim F, Hirscher M. Metal hydride materials for solid hydrogen storage: a review. Int J Hydrogen Energy 2007;32(9):1121–40. https://doi.org/10.1016/j.ijhydene.2006.11.022.
[37] Ley MB, Jepsen LH, Lee YS, Cho YW, Von Colbe JMB, Dornheim M, Jensen TR. Complex hydrides for hydrogen storage–new perspectives. Mater Today 2014;17(3):122–8. https://doi.org/10.1016/j.mattod.2014.02.013.
[38] Li C, Peng P, Zhou DW, Wan L. Research progress in LiBH4 for hydrogen storage: a review. Int J Hydrogen Energy 2011;36(22):14512–26. https://doi.org/10.1016/j.ijhydene.2011.08.030.
[39] Li HW, Akiba E, Orimo SI. Comparative study on the reversibility of pure metal borohydrides. J Alloys Compd 2013;580:S292–5. https://doi.org/10.1016/j.jallcom.2013.03.264.
[40] Sun T, Xiao F, Tang R, Wang Y, Dong H, Li Z, Zhu M. Hydrogen storage performance of nano Ni decorated LiBH4 on activated carbon prepared through organic solvent. J Alloys Compd 2014;612:287–92. https://doi.org/10.1016/j.jallcom.2014.05.134.
[41] Lombardo L, Yang H, Züttel A. Study of borohydride ionic liquids as hydrogen storage materials. J Energy Chem 2019;33:17–21. https://doi.org/10.1016/j.jechem.2018.08.011.
[42] Salmi T, Russo V. Reaction engineering approach to the synthesis of sodium borohydride. Chem Eng Sci 2019;199:79–87. https://doi.org/10.1016/j.ces.2019.01.007.
[43] Lee J, Shin H, Choi KS, Lee J, Choi JY, Yu HK. Carbon layer supported nickel catalyst for sodium borohydride (NaBH4) dehydrogenation. Int J Hydrogen Energy 2019;44(5):2943–50. https://doi.org/10.1016/j.ijhydene.2018.11.218.
[44] Himmelberger DW, Alden LR, Bluhm ME, Sneddon LG. Ammonia borane hydrogen release in ionic liquids. Inorg Chem 2009;48(20):9883–9. https://doi.org/10.1021/ic901560h.
[45] Chen W, Huang Z, Wu G, He T, Li Z, Chen J, Chen P. Guanidinium octahydrotriborate: an ionic liquid with high hydrogen storage capacity. J Mater Chem 2015;3(21):11411–6. https://doi.org/10.1039/C5TA01158B.
[46] Bartela Ł. A hybrid energy storage system using compressed air and hydrogen as the energy carrier. Energy 2020;196:117088. https://doi.org/10.1016/j.energy.2020.117088.
[47] Xiao R, Tian G, Hou Y, Chen S, Cheng C, Chen L. Effects of cooling-recovery venting on the performance of cryo-compressed hydrogen storage for automotive applications. Appl Energy 2020;269:115143. https://doi.org/10.1016/j.apenergy.2020.115143.
[48] Aceves SM, Berry GD, Martinez-Frias J, Espinosa-Loza F. Vehicular storage of hydrogen in insulated pressure vessels. Int J Hydrogen Energy 2006;31(15):2274–83. https://doi.org/10.1016/j.ijhydene.2006.02.019.
[49] Ahluwalia RK, Peng JK. Dynamics of cryogenic hydrogen storage in insulated pressure vessels for automotive applications. Int J Hydrogen Energy 2008;33(17):4622–33. https://doi.org/10.1016/j.ijhydene.2008.05.090.
[50] Aceves SM, Espinosa-Loza F, Ledesma-Orozco E, Ross TO, Weisberg AH, Brunner TC, Kircher O. High-density automotive hydrogen storage with cryogenic capable pressure vessels. Int J Hydrogen Energy 2010;35(3):1219–26. https://doi.org/10.1016/j.ijhydene.2009.11.069.
[51] Hua TQ, Ahluwalia RK, Peng JK, Kromer M, Lasher S, McKenney K, Sinha J. Technical assessment of compressed hydrogen storage tank systems for automotive applications. Int J Hydrogen Energy 2011;36(4):3037–49. https://doi.org/10.1016/j.ijhydene.2010.11.090.
[52] Cardella U, Decker L, Klein H. Roadmap to economically viable hydrogen liquefaction. Int J Hydrogen Energy 2017;42(19):13329–38. https://doi.org/10.1016/j.ijhydene.2017.01.068.
[53] Sadaghiani MS, Mehrpooya M. Introducing and energy analysis of a novel cryogenic hydrogen liquefaction process configuration. Int J Hydrogen Energy 2017;42(9):6033–50. https://doi.org/10.1016/j.ijhydene.2017.01.136.
[54] Reddi K, Elgowainy A, Rustagi N, Gupta E. Techno-economic analysis of conventional and advanced high-pressure tube trailer configurations for compressed hydrogen gas transportation and refueling. Int J Hydrogen Energy 2018;43(9):4428–38. https://doi.org/10.1016/j.ijhydene.2018.01.049.
[55] Petitpas G, Aceves SM. Liquid hydrogen pump performance and durability testing through repeated cryogenic vessel filling to 700 bar. Int J Hydrogen Energy 2018;43(39):18403–20. https://doi.org/10.1016/j.ijhydene.2018.08.097.
[56] Petitpas G, Moreno-Blanco J, Espinosa-Loza F, Aceves SM. Rapid high density cryogenic pressure vessel filling to 345 bar with a liquid hydrogen pump. Int J Hydrogen Energy 2018;43(42):19547–58. https://doi.org/10.1016/j.ijhydene.2018.08.139.

[57] Moreno-Blanco J, Petitpas G, Espinosa-Loza F, Elizalde-Blancas F, Martinez-Frias J, Aceves SM. The storage performance of automotive cryo-compressed hydrogen vessels. Int J Hydrogen Energy 2019;44(31):16841–51. https://doi.org/10.1016/j.ijhydene.2019.04.189.
[58] Yanxing Z, Maoqiong G, Yuan Z, Xueqiang D, Jun S. Thermodynamics analysis of hydrogen storage based on compressed gaseous hydrogen, liquid hydrogen and cryo-compressed hydrogen. Int J Hydrogen Energy 2019;44(31):16833–40. https://doi.org/10.1016/j.ijhydene.2019.04.207.
[59] Ariharan A, Ramesh K, Vinayagamoorthi R, Rani MS, Viswanathan B, Ramaprabhu S, Nandhakumar V. Biomass derived phosphorous containing porous carbon material for hydrogen storage and high-performance supercapacitor applications. J Energy Storage 2021;35:102185. https://doi.org/10.1016/j.est.2020.102185.
[60] Heo YJ, Park SJ. Synthesis of activated carbon derived from rice husks for improving hydrogen storage capacity. J Ind Eng Chem 2015;31:330–4. https://doi.org/10.1016/j.jiec.2015.07.006.
[61] Sethia G, Sayari A. Activated carbon with optimum pore size distribution for hydrogen storage. Carbon 2016;99:289–94. https://doi.org/10.1016/j.carbon.2015.12.032.
[62] Xiao Y, Dong H, Long C, Zheng M, Lei B, Zhang H, Liu Y. Melaleuca bark based porous carbons for hydrogen storage. Int J Hydrogen Energy 2014;39(22):11661–7. https://doi.org/10.1016/j.ijhydene.2014.05.134.
[63] Samantaray SS, Mangisetti SR, Ramaprabhu S. Investigation of room temperature hydrogen storage in biomass derived activated carbon. J Alloys Compd 2019;789:800–4. https://doi.org/10.1016/j.jallcom.2019.03.110.
[64] González-Navarro MF, Giraldo L, Moreno-Piraján JC. Preparation and characterization of activated carbon for hydrogen storage from waste African oil-palm by microwave-induced LiOH basic activation. J Anal Appl Pyrol 2014;107:82–6. https://doi.org/10.1016/j.jaap.2014.02.006.
[65] Üner O. Hydrogen storage capacity and methylene blue adsorption performance of activated carbon produced from Arundo donax. Mater Chem Phys 2019;237:121858. https://doi.org/10.1016/j.matchemphys.2019.121858.
[66] Zhang H, Zhu Y, Liu Q, Li X. Preparation of porous carbon materials from biomass pyrolysis vapors for hydrogen storage. Appl Energy 2022;306:118131. https://doi.org/10.1016/j.apenergy.2021.118131.
[67] Huang CC, Chen HM, Chen CH. Hydrogen adsorption on modified activated carbon. Int J Hydrogen Energy 2010;35(7):2777–80. https://doi.org/10.1016/j.ijhydene.2009.05.016.
[68] Gogotsi Y, Portet C, Osswald S, Simmons JM, Yildirim T, Laudisio G, Fischer JE. Importance of pore size in high-pressure hydrogen storage by porous carbons. Int J Hydrogen Energy 2009;34(15):6314–9. https://doi.org/10.1016/j.ijhydene.2009.05.073.
[69] Wang Z, Sun L, Xu F, Zhou H, Peng X, Sun D, Du Y. Nitrogen-doped porous carbons with high performance for hydrogen storage. Int J Hydrogen Energy 2016;41(20):8489–97. https://doi.org/10.1016/j.ijhydene.2016.03.023.
[70] Hu W, Li Y, Zheng M, Xiao Y, Dong H, Liang Y, Liu Y. Degradation of biomass components to prepare porous carbon for exceptional hydrogen storage capacity. Int J Hydrogen Energy 2021;46(7):5418–26. https://doi.org/10.1016/j.ijhydene.2020.11.015.
[71] Musyoka NM, Wdowin M, Rambau KM, Franus W, Panek R, Madej J, Czarna-Juszkiewicz D. Synthesis of activated carbon from high-carbon coal fly ash and its hydrogen storage application. Renew Energy 2020;155:1264–71. https://doi.org/10.1016/j.renene.2020.04.003.
[72] Kostoglou N, Koczwara C, Stock S, Tampaxis C, Charalambopoulou G, Steriotis T, Mitterer C. Nanoporous polymer-derived activated carbon for hydrogen adsorption and electrochemical energy storage. Chem Eng J 2022;427:131730. https://doi.org/10.1016/j.cej.2021.131730.
[73] Peng Z, Xu Y, Luo W, Wang C, Ma L. Conversion of biomass wastes into activated carbons by chemical activation for hydrogen storage. ChemistrySelect 2020;5(36):11221–8. https://doi.org/10.1002/slct.202000877.
[74] Zhao W, Luo L, Wang H, Fan M. Synthesis of bamboo-based activated carbons with super-high specific surface area for hydrogen storage. Bioresources 2017;12(1):1246–62.
[75] Bader N, Zacharia R, Abdelmottaleb O, Cossement D. How the activation process modifies the hydrogen storage behavior of biomass-derived activated carbons. J Porous Mater 2018;25(1):221–34. https://doi.org/10.1007/s10934-017-0436-8.
[76] Bicil Z, Dogan M. Characterization of activated carbons prepared from almond shells and their hydrogen storage properties. Energy Fuels 2021;35(12):10227–40. https://doi.org/10.1021/acs.energyfuels.1c00795.
[77] Musyoka NM, Mutuma BK, Manyala N. Onion-derived activated carbons with enhanced surface area for improved hydrogen storage and electrochemical energy application. RSC Adv 2020;10(45):26928–36. https://doi.org/10.1039/D0RA04556J.
[78] Rowlandson JL, Edler KJ, Tian M, Ting VP. Toward process-resilient lignin-derived activated carbons for hydrogen storage applications. ACS Sustainable Chem Eng 2020;8(5):2186–95. https://doi.org/10.1021/acssuschemeng.9b05869.
[79] Arshad SHM, Ngadi N, Aziz AA, Amin NS, Jusoh M, Wong S. Preparation of activated carbon from empty fruit bunch for hydrogen storage. J Energy Storage 2016;8:257–61. https://doi.org/10.1016/j.est.2016.10.001.
[80] Rambau KM, Musyoka NM, Manyala N, Ren J, Langmi HW. Mechanochemical approach in the synthesis of activated carbons from waste tyres and its hydrogen storage applications. Mater Today Proc 2018;5(4):10505–13. https://doi.org/10.1016/j.matpr.2017.12.382.
[81] Fomkin A, Pribylov A, Men'shchikov I, Shkolin A, Aksyutin O, Ishkov A, Khozina E. Adsorption-based hydrogen storage in activated carbons and model carbon structures. Reactions 2021;2(3):209–26. https://doi.org/10.3390/reactions2030014.
[82] Ramesh T, Rajalakshmi N, Dhathathreyan KS. Synthesis and characterization of activated carbon from jute fibers for hydrogen storage. Renewable Energy and Environmental Sustainability 2017;2:4. https://doi.org/10.1051/rees/2017001.
[83] Granitzer P, Rumpf K. Porous silicon—a versatile host material. Materials 2010;3(2):943–98. https://doi.org/10.3390/ma3020943.
[84] Sahoo MK, Kale P. Integration of silicon nanowires in solar cell structure for efficiency enhancement: a review. Journal of Materiomics 2019;5(1):34–48. https://doi.org/10.1016/j.jmat.2018.11.007.
[85] Sahoo MK, Kale P. Restructured porous silicon for solar photovoltaic: a review. Microporous Mesoporous Mater 2019;289:109619. https://doi.org/10.1016/j.micromeso.2019.109619.
[86] Muduli RC, Sahoo MK, Kale P. Wetting behavior of silicon nanowires array fabricated by Metal-assisted chemical etching. Mater Today Proc 2022. https://doi.org/10.1016/j.matpr.2022.04.635.
[87] Mikolajick T, Heinzig A, Trommer J, Pregl S, Grube M, Cuniberti G, Weber WM. Silicon nanowires—a versatile

technology platform. Phys Status Solidi Rapid Res Lett 2013;7(10):793–9. https://doi.org/10.1002/pssr.201307247.
[88] Samantaray SS, Sangeetha V, Abinaya S, Ramaprabhu S. Diatom frustule-graphene based nanomaterial for room temperature hydrogen storage. Int J Hydrogen Energy 2020;45(1):764–73. https://doi.org/10.1016/j.ijhydene.2019.10.155.
[89] González I, De Santiago F, Arellano LG, Miranda Á, Trejo A, Salazar F, Cruz-Irisson M. Theoretical modelling of porous silicon decorated with metal atoms for hydrogen storage. Int J Hydrogen Energy 2020;45(49):26321–33. https://doi.org/10.1016/j.ijhydene.2020.05.097.
[90] Kassaoui ME, Houmad M, Lakhal M, Benyoussef A, El Kenz A, Loulidi M. Hydrogen storage in lithium, sodium and magnesium-decorated on tetragonal silicon carbide. Int J Hydrogen Energy 2021;46(47):24190–201. https://doi.org/10.1016/j.ijhydene.2021.04.183.
[91] Boaks M, Schubert PJ. Kinetics of hydrogen storage on catalytically-modified porous silicon. J Catal 2019;371:81–7. https://doi.org/10.1016/j.jcat.2019.01.033.
[92] Goudarziafshar H, Abdolmaleki M, Moosavi-zare AR, Soleymanabadi H. Hydrogen storage by Ni-doped silicon carbide nanocage: a theoretical study. Phys E Low-dimens Syst Nanostruct 2018;101:78–84. https://doi.org/10.1016/j.physe.2018.03.001.
[93] Tabtimsai C, Ruangpornvisuti V, Tontapha S, Wanno B. A DFT investigation on group 8B transition metal-doped silicon carbide nanotubes for hydrogen storage application. Appl Surf Sci 2018;439:494–505. https://doi.org/10.1016/j.apsusc.2017.12.255.
[94] Liu F, Zhao Y, Hou H, Zhao Y, Wang Z, Huang Z. Enhanced hydrogen storage performance of Cu3 (BTC) 2 in situ inserted with few-layer silicon-based nanosheets. Int J Hydrogen Energy 2022;47(62):26537–48. https://doi.org/10.1016/j.ijhydene.2021.10.109.
[95] Li H, Retita I, Huang J, Chan SLI. Hydrogen storage capability of porous silicon powder fabricated from Al–Si alloy. Mater Chem Phys 2022;276:125405. https://doi.org/10.1016/j.matchemphys.2021.125405.
[96] Zhang Q, Huang Y, Ma T, Li K, Ye F, …, Wang X, et al. Facile synthesis of small MgH2 nanoparticles confined in different carbon materials for hydrogen storage. J Alloy Compd 2020;825:153953. https://doi.org/10.1016/j.jallcom.2020.153953.
[97] Zhu W, Panda S, Lu C, Ma Z, Khan D, Dong J, Zou J. Using a self-assembled two-dimensional MXene-based catalyst (2D-Ni@ Ti3C2) to enhance hydrogen storage properties of MgH2. ACS Appl Mater Interfaces 2020;12(45):50333–43. https://doi.org/10.1021/acsami.0c12767.
[98] Hu M, Xie X, Chen M, Zhu C, Liu T. TiCX-decorated Mg nanoparticles confined in carbon shell: preparation and catalytic mechanism for hydrogen storage. J Alloys Compd 2020;817:152813. https://doi.org/10.1016/j.jallcom.2019.152813.
[99] Liu T, Zhang T, Qin C, Zhu M, Li X. Improved hydrogen storage properties of Mg–V nanoparticles prepared by hydrogen plasma–metal reaction. J Power Sources 2011;196(22):9599–604. https://doi.org/10.1016/j.jpowsour.2011.07.078.
[100] Ali NA, Idris NH, Din MM, Mustafa NS, Sazelee NA, Yap FH, Ismail M. Nanolayer-like-shaped MgFe 2 O 4 synthesised via a simple hydrothermal method and its catalytic effect on the hydrogen storage properties of MgH 2. RSC Adv 2018;8(28):15667–74. https://doi.org/10.1039/C8RA02168F.
[101] Hosseini SE, Butler B. An overview of development and challenges in hydrogen powered vehicles. Int J Green Energy 2020;17(1):13–37. https://doi.org/10.1080/15435075.2019.1685999.
[102] Aziz M. Liquid hydrogen: a review on liquefaction, storage, transportation, and safety. Energies 2021;14(18):5917. https://doi.org/10.3390/en14185917.
[103] Broom DP, Webb CJ, Hurst KE, Parilla PA, Gennett T, Brown CM, Hirscher M. Outlook and challenges for hydrogen storage in nanoporous materials. Appl Phys A 2016;122(3):1–21. https://doi.org/10.1007/s00339-016-9651-4.
[104] Visaria M, Mudawar I, Pourpoint T, Kumar S. Study of heat transfer and kinetics parameters influencing the design of heat exchangers for hydrogen storage in high-pressure metal hydrides. Int J Heat Mass Tran 2010;53(9–10):2229–39. https://doi.org/10.1016/j.ijheatmasstransfer.2009.12.010.
[105] Niaz S, Manzoor T, Pandith AH. Hydrogen storage: materials, methods and perspectives. Renew Sustain Energy Rev 2015;50:457–69. https://doi.org/10.1016/j.rser.2015.05.011.
[106] Moradi R, Groth KM. Hydrogen storage and delivery: review of the state of the art technologies and risk and reliability analysis. Int J Hydrogen Energy 2019;44(23):12254–69. https://doi.org/10.1016/j.ijhydene.2019.03.041.
[107] Myers D.B., Ariff G.D., James B.D., Lettow J.S., Thomas C.E., Kuhn R.C. Cost and performance comparison of stationary hydrogen fueling appliances. The Hydrogen Program Office 2002. pg 1-8
[108] Rusman NAA, Dahari M. A review on the current progress of metal hydrides material for solid-state hydrogen storage applications. Int J Hydrogen Energy 2016;41(28):12108–26. https://doi.org/10.1016/j.ijhydene.2016.05.244.
[109] Aziz M, Oda T, Kashiwagi T. Comparison of liquid hydrogen, methylcyclohexane and ammonia on energy efficiency and economy. Energy Proc 2019;158:4086–91. https://doi.org/10.1016/j.egypro.2019.01.827.
[110] Choi M, Jung W, Lee S, Joung T, Chang D. Thermal efficiency and economics of a boil-off hydrogen Re-liquefaction system considering the energy efficiency design index for liquid hydrogen carriers. Energies 2021;14(15):4566. https://doi.org/10.3390/en14154566.
[111] Sdanghi G, Maranzana G, Celzard A, Fierro V. Review of the current technologies and performances of hydrogen compression for stationary and automotive applications. Renew Sustain Energy Rev 2019;102:150–70. https://doi.org/10.1016/j.rser.2018.11.028.
[112] Petitpas G, Aceves SM, Matthews MJ, Smith JR. Para-H2 to ortho-H2 conversion in a full-scale automotive cryogenic pressurized hydrogen storage up to 345 bar. Int J Hydrogen Energy 2014;39(12):6533–47. https://doi.org/10.1016/j.ijhydene.2014.01.205.
[113] Ramirez-Vidal P, Canevesi RL, Sdanghi G, Schaefer S, Maranzana G, Celzard A, Fierro V. A step forward in understanding the hydrogen adsorption and compression on activated carbons. ACS Appl Mater Interfaces 2021;13(10):12562–74. https://doi.org/10.1021/acsami.0c22192.
[114] Hermosilla-Lara G, Momen G, Marty PH, Le Neindre B, Hassouni K. Hydrogen storage by adsorption on activated carbon: investigation of the thermal effects during the charging process. Int J Hydrogen Energy 2007;32(10–11):1542–53. https://doi.org/10.1016/j.ijhydene.2006.10.048.
[115] Lototskyy MV, Yartys VA, Pollet BG, Bowman Jr RC. Metal hydride hydrogen compressors: a review. Int J Hydrogen Energy 2014;39(11):5818–51. https://doi.org/10.1016/j.ijhydene.2014.01.158.

[116] Kaur M, Pal K. Review on hydrogen storage materials and methods from an electrochemical viewpoint. J Energy Storage 2019;23:234–49. https://doi.org/10.1016/j.est.2019.03.020.
[117] Bobbitt NS, Snurr RQ. Molecular modelling and machine learning for high-throughput screening of metal-organic frameworks for hydrogen storage. Mol Simulat 2019;45(14–15):1069–81. https://doi.org/10.1080/08927022.2019.1597271.
[118] Rahimi M, Abbaspour-Fard MH, Rohani A. Machine learning approaches to rediscovery and optimization of hydrogen storage on porous bio-derived carbon. J Clean Prod 2021;329:129714. https://doi.org/10.1016/j.jclepro.2021.129714.
[119] Jia Y, Sun C, Shen S, Zou J, Mao SS, Yao X. Combination of nanosizing and interfacial effect: future perspective for designing Mg-based nanomaterials for hydrogen storage. Renew Sustain Energy Rev 2015;44:289–303. https://doi.org/10.1016/j.rser.2014.12.032.
[120] Wu C, Cheng HM. Effects of carbon on hydrogen storage performances of hydrides. J Mater Chem 2010;20(26):5390–400. https://doi.org/10.1039/B926880D.
[121] Zhao L, Xu F, Zhang C, Wang Z, Ju H, Gao X, Liu Z. Enhanced hydrogen storage of alanates: recent progress and future perspectives. Prog Nat Sci: Mater Int 2021;31(2):165–79. https://doi.org/10.1016/j.pnsc.2021.01.007.